

Aerobic Biotransformation and Defluorination of Fluoroalkylether Substances (ether PFAS): Substrate Specificity, Pathways, and Applications

Bosen Jin, Yiwen Zhu, Weiyang Zhao, Zekun Liu, Shun Che, Kunpeng Chen, Ying-Hsuan Lin, Jinyong Liu, and Yujie Men*



Cite This: *Environ. Sci. Technol. Lett.* 2023, 10, 755–761



Read Online

ACCESS |

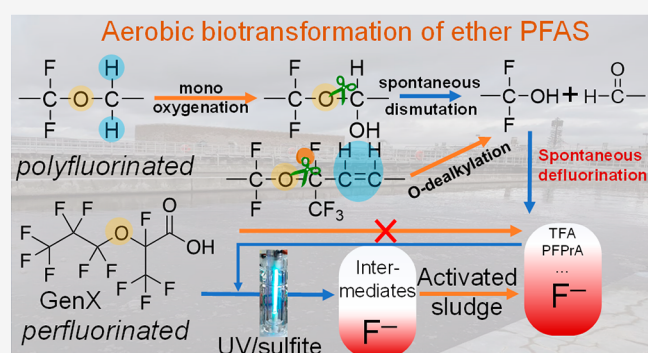
Metrics & More

Article Recommendations

Supporting Information

ABSTRACT: Fluoroalkylether substances (ether PFAS) constitute a large group of emerging PFAS with uncertain environmental fate. Among them, GenX is the well-known alternative to perfluorooctanoic acid and one of the six proposed PFAS to be regulated by the U.S. Environmental Protection Agency. This study investigated the structure–biodegradability relationship for 12 different ether PFAS with a carboxylic acid headgroup in activated sludge communities. Only polyfluorinated ethers with at least one $-\text{CH}_2-$ moiety adjacent to or a $\text{C}=\text{C}$ bond in the proximity of the ether bond underwent active biotransformation via oxidative and hydrolytic O-dealkylation. The bioreactions at ether bonds led to the formation of unstable fluoroalcohol intermediates subject to spontaneous defluorination. We further demonstrated that this aerobic biotransformation/defluorination could complement the advanced reduction process in a treatment train system to achieve more cost-effective treatment for GenX and other recalcitrant perfluorinated ether PFAS. These findings provide essential insights into the environmental fate of ether PFAS, the design of biodegradable alternative PFAS, and the development of cost-effective ether PFAS treatment strategies.

KEYWORDS: ether PFAS, structural specificity, GenX, aerobic biotransformation, defluorination, PFAS treatment train



INTRODUCTION

Per- and polyfluoroalkyl substances (PFAS) have attracted more public attention over the past several decades.¹ PFAS-containing products have been extensively employed in diverse applications across commerce and industry.² As research continuously demonstrates their persistence in the environment¹ and bioaccumulation and toxicity in living organisms,^{3–5} many legacy PFAS, such as perfluorooctanoic acid (PFOA) and perfluorooctanesulfonic acid (PFOS), have been gradually phased out.⁶ In the meantime, fluoroalkylether substances (ether PFAS) have been designed and produced as alternative PFAS, including GenX [hexafluoropropylene oxide dimer acid (HFPO-DA)] and F-53B [6:2 chlorinated polyfluoroalkyl ether sulfonate (6:2 Cl-PFESA)].⁷ Ether PFAS is one of the most important groups within the large PFAS family.^{8,9}

In March 2023, the government planned to allocate approximately \$9 billion in funding to help reduce the PFAS levels in drinking water over five years in the United States.¹⁰ In response, the U.S. Environmental Protection Agency has proposed the National Primary Drinking Water Regulation (NPDWR) to enforce strict maximum contaminant levels for six PFAS in drinking water, including GenX. Those actions

have drawn more public attention to ether PFAS.¹¹ Notably, a variety of ether PFAS, including novel ones, have been detected in soil, wastewater, surface water, groundwater, and human blood.^{6,7,12–15} Consequently, understanding the environmental fate of ether PFAS is crucial for assessing their potential risks and developing effective mitigation strategies.¹

Although some studies have investigated the environmental occurrence and fate of some emerging ether PFAS,^{7,12–18} a significant knowledge gap remains regarding a systematic understanding of the biodegradability of various ether PFAS structures. Critical questions have not yet been tackled, such as which structures could be biotransformed and through what biotransformation pathways. More importantly, in addition to elucidating the fate of ether PFAS in microbially active

Received: June 19, 2023

Revised: July 27, 2023

Accepted: July 31, 2023

Published: August 7, 2023



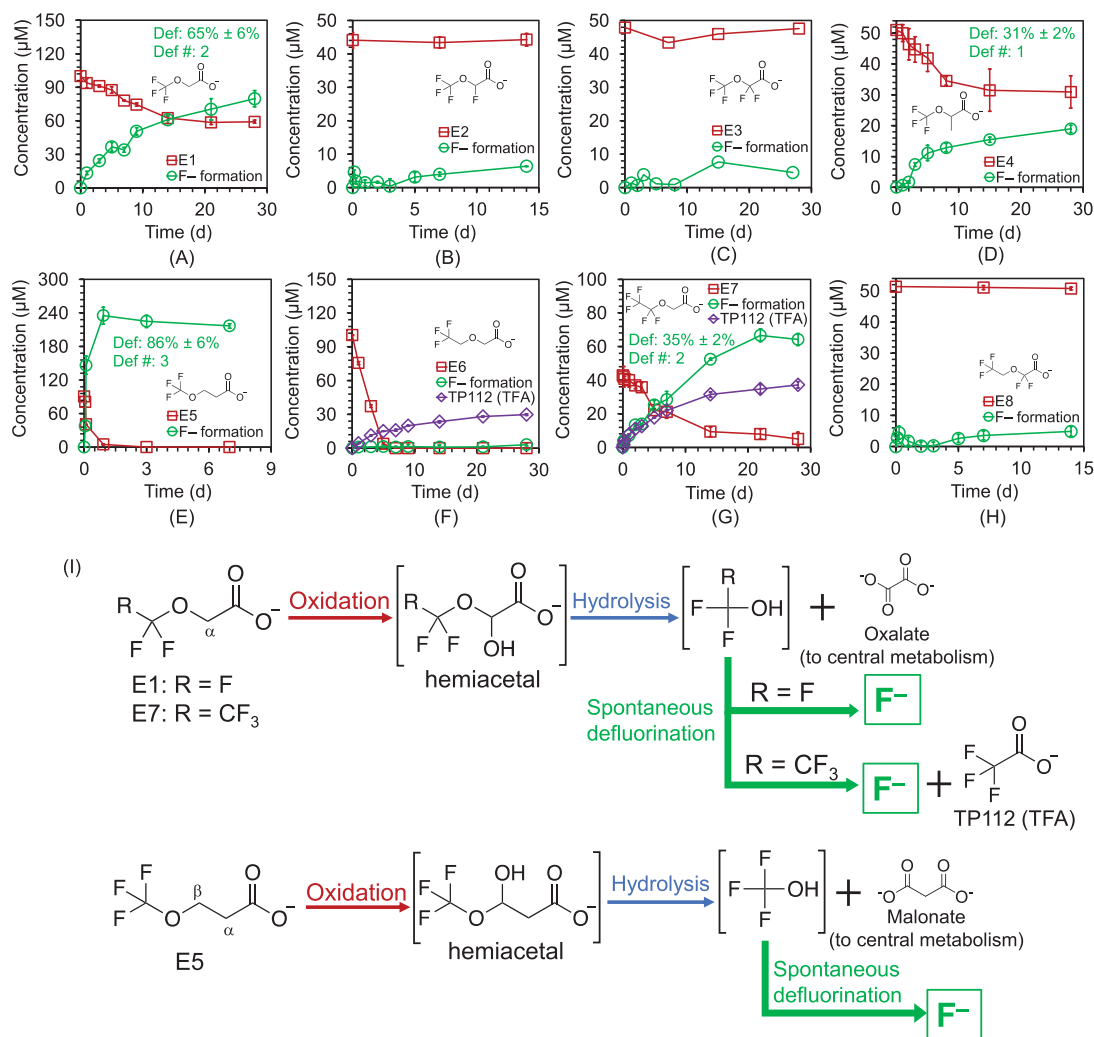


Figure 1. (A–H) Aerobic biotransformation and defluorination of E1–E8, respectively. All of the parent compounds and TPs were presented as the sum of extracellular and cell-associated concentrations (with the reference compound available) or peak areas (with the reference compound unavailable) in the same sample taken over a time course. No transformation or fluoride formation was observed in the abiotic controls (Figure S1). (I) Proposed aerobic biotransformation and defluorination pathways of E1, E5, and E7 (in brackets are transient intermediates that could not be detected).

environments, a long-standing unanswered question is whether microbial processes could be harnessed to enhance the relatively low chemical treatability of ether PFAS,¹⁹ thus reducing treatment costs.

To address these questions, in this study, we comprehensively investigated the aerobic biotransformation and defluorination of a series of ether PFAS, elucidated the biotransformation pathways, and provided the specific ether PFAS structures susceptible to biotransformation. On the basis of the structure–biodegradability relationship, we further integrated the aerobic biotransformation with the advanced reduction treatment and demonstrated enhanced defluorination for several perfluorinated ether PFAS, including GenX. Our findings contribute to a deeper understanding of ether PFAS biotransformation in the environment and the development of more cost-effective remediation strategies for these persistent and hazardous compounds.

MATERIALS AND METHODS

Chemicals. We investigated 12 ether PFAS [Figures 1 and 2 (see their detailed information in Table S1)], including eight

structurally similar C_3 – C_4 ether PFAS (E1–E8) and four C_5 – C_6 structures, including GenX and its analogues (E9–E12). Some of them, such as GenX and E3, have already been detected in aquatic environments, while some serve as building blocks for the synthesis of fluoropolymers and other fluorochemicals and may also be detected in the environment.^{18,20,21}

Aerobic Biotransformation Experiments. The activated sludge community freshly taken from a local municipal wastewater treatment plant (WWTP) (~ 4400 mg/L as total suspended solids) was added (50 mL) to each 150 mL loosely capped batch reactor spiked with individual ether PFAS at an initial concentration of $50 \mu\text{M}$ except for E1, E5, E6, and E11, whose initial concentration was $100 \mu\text{M}$ due to their detection limit being higher than those of the other seven ether PFAS. The initial concentration of $100 \mu\text{M}$ would allow a more accurate analysis of the parent compound and the potential transformation products. Reactors were incubated at room temperature for ≤ 28 days on a shaker (150 rpm) with a dissolved oxygen level of >3 mg/L. The dissolved oxygen levels were determined by a Hach DO probe. As in previous

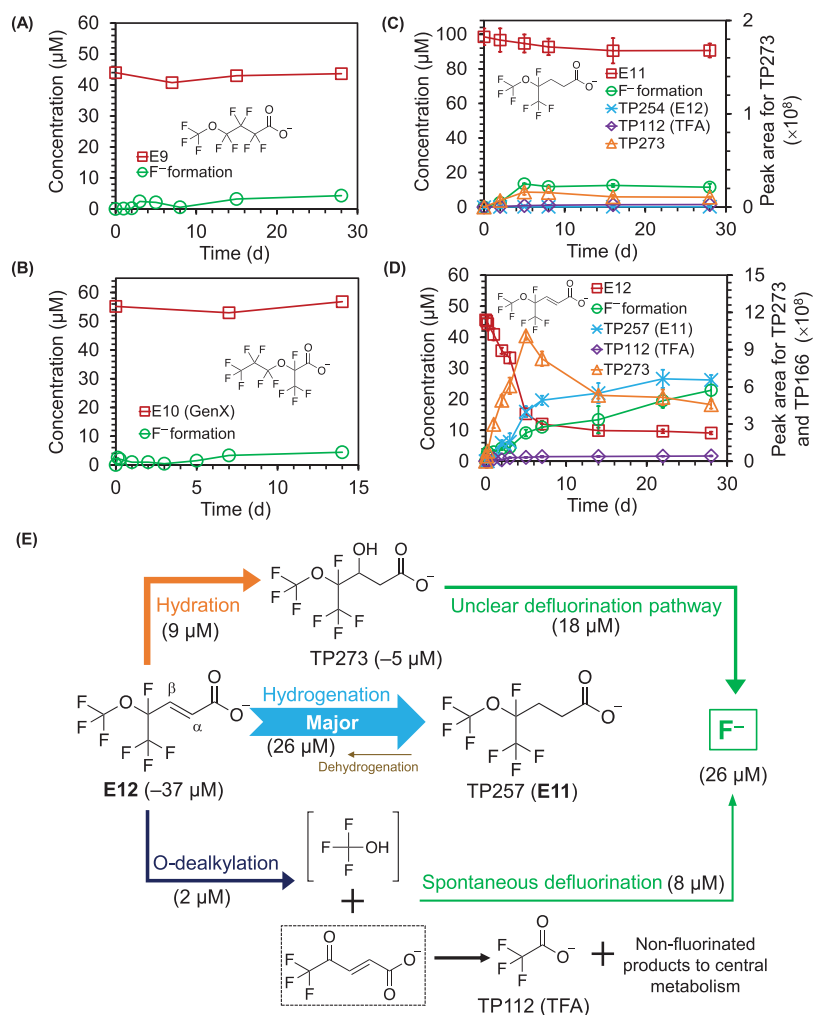


Figure 2. (A–D) Aerobic biotransformation and defluorination of E9–E12, respectively (all of the parent compounds and TPs are presented as the total concentration or peak area in the supernatant and associated with cells). (E) Proposed aerobic biotransformation and defluorination pathways of E11 and E12 (in the dashed box is shown the undetected proposed intermediate; in brackets is shown the transient intermediate that cannot be detected).

studies,^{22,23} methanol and ammonium were added as the supplemental carbon and nitrogen source, respectively, to each reactor to sustain the sludge activity after 3 days. Abiotic controls were also performed in the same setup, which included autoclaved sludge (121 °C, 40 min) and autoclaved sludge filtrate (0.22 μm). In addition, the sludge-only controls without the spike of ether PFAS were also set up to account for the F⁻ concentration in the sludge matrix, where the level of F⁻ fluctuated with the maximum formation of ~10 μM during the incubation period (Figure S1A). Thus, we consider only F⁻ levels of >10 μM in the experimental samples as active defluorination.

For the integrated chemical and biological transformation experiments, the effluent from the advanced reduction treatment using hydrated electrons in ultraviolet (UV)/sulfite reactors¹⁹ (see the Supplementary Methods in the Supporting Information for the photochemical reactor setup) was added (25 mL) to 25 mL of a 2-fold concentrated activated sludge community (by removing 25 mL of the supernatant after settling down 50 mL of sludge) in the 150 mL batch reactors with the same incubation conditions.

Samples (~1.5 mL) were taken at multiple time points during the aforementioned biotransformation experiments and

centrifuged at 13 000 rpm for 20 min. The supernatant (~1.2 mL) was collected to measure the parent compound and transformation products (TPs). The cell-associated parent compound and TPs were extracted using 1.5 mL of methanol with 1% NH₄OH (see the Supplementary Methods). The samples were stored at 4 °C and analyzed within 3 weeks.

Fluoride Measurement. The HQ30D Portable Multi Meter (HACH) connected with an ion-selective electrode (ISE, HACH) was used for the fluoride ion (F⁻) measurement. Fluoride Ionic Strength Adjustor (ISA) powder was added to eliminate the interference from aluminum and iron in the matrix before detection. The limit of quantification (LOQ) is 0.01 mg/L (~0.5 μM). The fluoride measurement in the same matrix was cross-validated using ion chromatography in a previous study.²² The defluorination degree (Def %) was calculated using the equation

$$\text{Def \%} = \frac{\text{maximum F}^{-} \text{ formation } (\mu\text{M})}{\text{removed concentration } (\mu\text{M}) \times \text{no. of F in one molecule}} \times 100\%$$

Analytical Methods. An ultra-high-performance liquid chromatograph coupled with a high-resolution mass spectrometer (UHPLC-HRMS/MS, Q Exactive, Thermo Fisher

Scientific) was employed for the detection of parent compounds and TPs. A Hypersil Gold column (particle size of 1.9 μm , 2.1 mm \times 100 mm, Thermo Fisher Scientific) was used for UHPLC separation. For HRMS detection, the negative electrospray ionization mode (ESI⁻) was used with a resolution of 70 000 @ m/z 200 for the full scan (m/z 70–1050) and 17 500 @ m/z 200 for the data-dependent MS² scan. For TP identification, we applied both suspect and nontarget screening. Details are included in the [Supplementary Methods](#).

RESULTS AND DISCUSSION

Substrate Specificity of Aerobic Biotransformation and Defluorination of Ether PFAS. For short-chain (C3 to C4) ether PFAS, the aerobic biotransformation was observed for only those with at least one nonfluorinated carbon between the ether and the carboxyl group (i.e., E1 and E4–E7) ([Figure 1A–H](#) and [Figure S1](#)). This is similar to our previous finding that active aerobic biotransformation of short-chain polyfluorocarboxylic acids (PFCAs) required nonfluorinated carbon next to the carboxylic group.²² A previous study reported that 2H-3:2PFECA (C₃F₇OCHF⁻COO⁻) with a monofluorinated (-CHF-) moiety next to the ether bond also exhibited very slow aerobic biotransformation via a similar O-dealkylation pathway with a small amount of perfluoropropionic acid (PFPrA) being formed.¹⁷ It is consistent with our observation for E2 with the same -CHF- moiety, which did not exhibit notable parent compound decay or defluorination during the much shorter incubation period (14 days vs 84 days in that study).

For the five biotransformed ether PFAS structures, the aerobic biotransformation was initiated by the oxidation (i.e., hydroxylation) at the nonfluorinated carbon next to the ether group, forming an unstable hemiacetal intermediate, which spontaneously dismutates into an alcohol product and an aldehyde product. This pathway of ether scission has been observed in various microorganisms according to the detection of the expected end products.^{24–29} It could be catalyzed by monooxygenases and has been widely reported in the aerobic biodegradation of dialkyl ethers, chlorinated dialkyl ethers [e.g., bis(2-chloroethyl) ether], and 1,4-dioxane.^{24,25,28,30} The aldehyde product from the hemiacetal intermediate could be further oxidized, forming a carboxyl group.^{29,30} The nonfluorinated dicarboxylic acid products (e.g., oxalate from E1 and E7 and malonate from E5) could enter the central metabolic pathway ([Figure 1I](#)).

As for the alcohol product, it can also be further oxidized. Spontaneous defluorination occurs when fluorine substitutions are at the alcohol carbon (-CF₂OH) ([Figure 1I](#)). This fluoroalcohol structure is unstable and undergoes spontaneous HF elimination followed by hydrolysis, leading to the cleavage of all C–F bonds on the alcohol carbon ([Figure 1I](#) and [Figure S2](#)). This explains why defluorination was observed for E1, E4, E5, and E7 but not for E6, which was converted into an alcohol intermediate with a -CH₂OH moiety instead of a -CF₂OH moiety. Further oxidation of the alcohol intermediate of E6 (2,2,2-trifluoroethanol, undetectable via LC-HRMS/MS) led to the formation of trifluoroacetate (TFA) that was resistant to biodegradation and accumulated as the end product ([Figure 1F](#) and [Figure S3](#)). As only the C–F bonds next to the ether bond were spontaneously cleaved, TFA was also the major product from E7 after the spontaneous defluorination. It was detected at the stoichiometric concentration (37.2 μM)

corresponding to the 37.9 μM removal of E7 and \sim 67 μM formation of F⁻ at the end of the incubation ([Figure 1G,I](#)).

The monooxygenation was faster for C4 structures (i.e., E5–E7) than for C3 structures (i.e., E1 and E4). The methyl branch in E4 led to slower defluorination. The parent compound removal of E4 (39.3%) was similar to that of E1 (40.9%), indicating that the initial hydroxylation of the parent compound was not affected by the methyl branch. The lower level of defluorination of E4 than of E1 was then likely due to a slower follow-up dismutation of the hydroxylation intermediate caused by the steric effect of the methyl group,³¹ rendering a slower release of fluoride.

For the longer-chain ether PFAS (i.e., E9–E12), not surprisingly, the two perfluorinated structures (i.e., E9 and E10, also known as GenX) did not show any biotransformation ([Figure 2A,B](#)). In contrast, the other two polyfluorinated structures (i.e., E11 and E12) exhibited biotransformation and defluorination ([Figure 2C,D](#)) but to different extents. E11 and E12 differ by only the saturation/unsaturation at the α - β position. However, with the unsaturated C=C bond, E12 exhibited 80% removal, whereas the removal of saturated E11 was only 8%, indicating that the C=C bond in E12 was more bioreactive than the C–C bond in E11. A majority (26 μM) of the removed E12 (37 μM) underwent hydrogenation, forming E11 within a week. The back transformation of E11 to E12 via dehydrogenation was much slower, rendering a low removal of E11. In addition to the nondefluorinating hydrogenation pathway, E12 (11 μM) underwent two defluorinating pathways according to the two identified transformation products, TP273 and TFA ([Figure 2C–E](#) and [Figure S4](#)). Of the 11 μM E12, \sim 2 μM was converted into TFA, possibly through hydrolytic O-dealkylation ([Figure 2E](#)), corresponding to the formation of 8 μM fluoride (four atoms of F released per TFA formed). Thus, the remaining 9 μM of E12 could be hydrated at the C=C bond, forming TP273, which was further transformed likely at the ether C, although the specific reactions remain unclear ([Figure 2D,E](#)). This led to continuous defluorination after E12's depletion and an additional 18 μM of fluoride release corresponding to \sim 5 μM TP273 removal (approximately four atoms of F cleaved from one TP273 molecule) ([Figure 2E](#)).

It is worth noting that the ether bond played a critical role in the defluorination of E11 and E12 as the respective structures without the ether bond, i.e., FTMePA [(CF₃)₂CFCH₂CH₂COOH] and FTMeUPA [(CF₃)₂CFCH=CHCOOH] did not exhibit any defluorination in the activated sludge community taken from the same WWTP.²³ FTMePA was resistant to biotransformation, while FTMeUPA underwent only hydrogenation forming FTMePA.²³ Although the major biotransformation route for E12 was also hydrogenation, the ether bond enabled alternative routes that led to the release of up to four F atoms per molecule of removed E12. Future studies could be done to enhance the defluorinating routes by identifying the microorganisms and enzymes responsible for the different pathways, stimulating the desired pathways and repressing the undesired ones.

Enhanced Defluorination of Recalcitrant Ether PFAS by the Chemical–Biological Treatment Train System. The highly and fully fluorinated ether PFAS, such as GenX and similar structures, was much more recalcitrant to biodegradation. Even chemical reductive degradation using UV (254 nm) and SO₃²⁻ (10 mM) at pH 9.5 showed sluggish defluorination (<50% after 48 h for GenX).¹⁹ This is because the F \rightarrow H

exchange products become more difficult to reduce. A combination with advanced chemical oxidation was suggested to achieve a higher level of defluorination.³² Alternatively, inspired by the structure specificity of aerobic biotransformation of ether PFAS identified above, the less fluorinated products with more C–H bonds could be further transformed and defluorinated by aerobic microbial communities.^{22,33} Using aerobic biological processes would be more cost-effective than chemical oxidation. To prove this concept, we used the same activated sludge community to treat the effluent of the UV/SO₃²⁻ system treating all five nonbiodegradable ether PFAS, including E10 (GenX), E2, E3, E8, and E9. An additional 11–28% defluorination was achieved by the aerobic biological post-treatment after 8 days for all five compounds (Figure 3A), while no F⁻ release was detected in the abiotic controls (Figure S5).

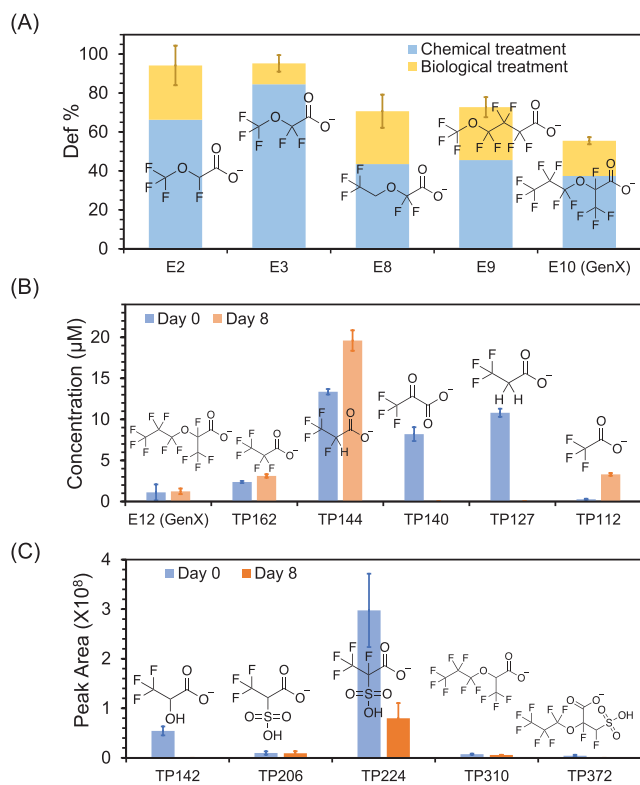


Figure 3. (A) Degree of defluorination of chemical and aerobic biological post-treatments for E2, E3, and E8–E10 (GenX). (B) Quantifiable TPs before and after the aerobic biological post-treatment of E10 (GenX) chemical treatment effluent. (C) Non-quantifiable TPs presented as peak areas before and after the post-aerobic biological treatment of E10 (GenX) chemical treatment effluent [Day 0, after the chemical treatment and before the aerobic biological post-treatment; Day 8, 8 days after the aerobic biological post-treatment; error bars represent the standard deviation ($n = 3$) (see Figure S6 for the LC-HRMS/MS detection of the non-quantifiable TPs)].

Expectedly, the additional defluorination mainly came from the aerobic biotransformation of chemical treatment products that contain the -CH₂- moiety next to the ether or carboxylic group (Figure 3B and Figures S6 and S7). With GenX as an example, in addition to trifluoropropionate (TP127), which is known to be completely defluorinated in activated sludge communities,²² the sulfonated products (TP224 and TP372)

(Figure 3C) were other chemical treatment products^{19,34} that were microbially transformed, via desulfonation^{35,36} or hydroxylation, forming unstable fluoroalcohol intermediates, hence contributing to the additional defluorination. The slight formation of PFPPrA (TP162) seemed to be a result of the O-dealkylation of TP372 (Figure 3B,C). In addition, trifluoroacetate (TFA) was formed via the nondefluorinating biotransformation of certain chemical treatment products, such as trifluoropyruvate (TP140), trifluorolactate (TP142), and sulfonated trifluoropropionate (TP206).

ENVIRONMENTAL IMPLICATIONS

This study demonstrates that the ether bond(s) in PFAS molecules could serve as a weak point for aerobic microorganisms to attack, thus playing critical roles in enhancing biodegradability and the defluorination potential. At least one -CH₂- moiety on the nonfluorinated side of the -O- bond is necessary to trigger an active microbial attack. Monooxygenation occurs at the -CH₂- moiety next to the -O- bond, forming an unstable hemiacetal intermediate, which undergoes O-dealkylation forming an alcohol and an aldehyde. Spontaneous defluorination will then happen to the alcohol product if the alcohol carbon is fluorinated (e.g., CF₃-OH and -CF₂-OH). Many microbial species possessing monooxygenases or cytochromes P-450 can cleave ether structures (both alkyl and aryl) via this oxidation pathway.²⁴ We previously discovered a β -oxidation-like pathway for polyfluorocarboxylic acids (PFCAs), CF₃(CF₂)_{*m*}(CH₂)_{*n*}COOH, where the defluorination could be observed for only an odd number of *n*. If an ether bond(s) were introduced into the PFCA structure, i.e., CF₃(CF₂)_{*m*}O(CH₂)_{*n*}COOH, the defluorination next to the ether bond will then always be triggered by the oxidative ether cleavage. In addition to the oxidative ether cleavage mechanism, we also observed hydrolytic O-dealkylation for an unsaturated ether PFAS structure (E12) that does not have a -CH₂- moiety next to the ether bond. The C=C bond makes the structure more biodegradable compared to its saturated counterpart. The ether bond in this structure further enables defluorination triggered by either direct hydrolytic O-dealkylation or hydration at the C=C bond. Both reactions have been proposed for ether cleavage in nonfluorinated unsaturated ether structures with the double bond on the ether carbon, such as vinyl ether and isochorismic acid with a -O-C=C- moiety.²⁴ The activated sludge community used in this study came from a typical municipal WWTP. Thus, similar biotransformation activities may be observed in other municipal WWTPs. Also, microorganisms in activated sludge communities commonly occur in natural environments, where similar biotransformation patterns may exist. However, biotransformation kinetics could vary, depending on the microbial abundance and activities. Thus, understanding the role played by ether bonds in the biodegradability of ether PFAS and the transformation mechanisms, particularly the structure–biodegradability relationship, can help predict the environmental fate of various ether PFAS structures that are being used and discharged into natural and engineered environments.^{2,21} It can also provide important guidance for the design of biodegradable alternative PFAS.

Furthermore, on the basis of the identified structure–biodegradability relationship, we demonstrated the concept of using a chemical–biological treatment train system to achieve enhanced destruction of ether PFAS that cannot be effectively treated by either method alone. Perfluorinated ether PFAS are

resistant to advanced oxidation by hydroxyl radicals.²¹ Advanced reduction by hydrated electrons reaches only <50% total defluorination for GenX and its derivatives due to the formation of more C–H bonds via the undesirable reductive defluorination pathway.¹⁹ Nevertheless, what is undesirable in chemical treatment is attractive to aerobic microorganisms. Up to 28% increase in the total defluorination could be achieved by aerobic biological post-treatment, where many chemical treatment products with a -CH₂- moiety were further biodegraded and defluorinated into short-chain perfluorinated acids. Compared to advanced oxidation processes (AOPs), which would result in the same short-chain perfluorinated end products,^{32,37} the biological post-treatment is more cost-effective, particularly when there is high-level nonfluorinated dissolved organic carbon in the matrix that may severely affect the AOP performance. After the aerobic biological post-treatment, although the defluorination of GenX was still incomplete, it simplified the major end products to three short-chain PFCAs (i.e., PFPrA, 2,3,3,3-tetrafluoropropionic acid, and TFA), which could be further degraded by a secondary advanced reduction treatment.^{38–40} TFA can be quickly and completely degraded by UV/sulfite treatment, while PFPrA and 2,3,3,3-tetrafluoropropionic acid may form the chemically stable trifluoropropionate,⁴⁰ which can be completely destroyed in another round of aerobic biological post-treatment.²² Thus, upon implementation of appropriate recirculation, the chemical–biological treatment train system could achieve nearly complete destruction of GenX and other structurally similar ether PFAS that show no or low-level destruction in biological and chemical treatment alone. This sheds light on the development of more cost-effective and environmentally friendly PFAS treatment strategies.

■ ASSOCIATED CONTENT

SI Supporting Information

The Supporting Information is available free of charge at <https://pubs.acs.org/doi/10.1021/acs.estlett.3c00411>.

Additional experimental details, materials, and methods; parent compound removal and fluoride ion formation in abiotic controls; LC-HRMS/MS chromatographs and full-scan and MS² spectra of TPs; and biological post-treatment performance for E2, E3, E8, and E9 (PDF)

■ AUTHOR INFORMATION

Corresponding Author

Yujie Men – Department of Chemical and Environmental Engineering, University of California, Riverside, California 92521, United States; orcid.org/0000-0001-9811-3828; Phone: (951) 827-1019; Email: yjmen@engr.ucr.edu

Authors

Bosen Jin – Department of Chemical and Environmental Engineering, University of California, Riverside, California 92521, United States; orcid.org/0000-0001-7659-3437

Yiwen Zhu – Department of Chemical and Environmental Engineering, University of California, Riverside, California 92521, United States

Weiyang Zhao – Department of Chemical and Environmental Engineering, University of California, Riverside, California 92521, United States

Zekun Liu – Department of Chemical and Environmental Engineering, University of California, Riverside, California 92521, United States

Shun Che – Department of Chemical and Environmental Engineering, University of California, Riverside, California 92521, United States

Kunpeng Chen – Department of Environmental Sciences, University of California, Riverside, California 92521, United States; orcid.org/0000-0002-9430-9257

Ying-Hsuan Lin – Department of Environmental Sciences, University of California, Riverside, California 92521, United States; orcid.org/0000-0001-8904-1287

Jinyong Liu – Department of Chemical and Environmental Engineering, University of California, Riverside, California 92521, United States; orcid.org/0000-0003-1473-5377

Complete contact information is available at:

<https://pubs.acs.org/10.1021/acs.estlett.3c00411>

Notes

The authors declare no competing financial interest.

■ ACKNOWLEDGMENTS

This work was supported by the Strategic Environmental Research and Development Program (Project ER20-1541 for B.J., Z.L., J.L., and Y.M. and Project ER23-3694 for Y.Z.) and the National Institute of Environmental Health Sciences (Grant R01ES032668 to S.C., W.Z., and Y.M.). Computations were performed using the computer clusters and data storage resources of the High-Performance Computer Cluster at the University of California, Riverside, which were funded by grants from the National Science Foundation (MRI-2215705 and MRI-1429826) and the National Institutes of Health (1S10OD016290-01A1).

■ REFERENCES

- (1) Evich, M. G.; Davis, M. J. B.; McCord, J. P.; Acrey, B.; Awkerman, J. A.; Knappe, D. R. U.; Lindstrom, A. B.; Speth, T. F.; Tebes-Stevens, C.; Strynar, M. J.; et al. Per- and polyfluoroalkyl substances in the environment. *Science* **2022**, *375* (6580), abg9065.
- (2) Gluge, J.; Scheringer, M.; Cousins, I. T.; DeWitt, J. C.; Goldenman, G.; Herzke, D.; Lohmann, R.; Ng, C. A.; Trier, X.; Wang, Z. An overview of the uses of per- and polyfluoroalkyl substances (PFAS). *Environ. Sci.: Processes Impacts* **2020**, *22* (12), 2345–2373.
- (3) Li, J.; Sun, J.; Li, P. Exposure routes, bioaccumulation and toxic effects of per- and polyfluoroalkyl substances (PFASs) on plants: A critical review. *Environ. Int.* **2022**, *158*, 106891.
- (4) Jin, B.; Mallula, S.; Golovko, S. A.; Golovko, M. Y.; Xiao, F. In Vivo generation of PFOA, PFOS, and other compounds from cationic and zwitterionic per- and polyfluoroalkyl substances in a terrestrial invertebrate (*Lumbricus terrestris*). *Environ. Sci. Technol.* **2020**, *54* (12), 7378–7387.
- (5) Dickman, R. A.; Aga, D. S. A review of recent studies on toxicity, sequestration, and degradation of per- and polyfluoroalkyl substances (PFAS). *J. Hazard. Mater.* **2022**, *436*, 129120.
- (6) Washington, J. W.; Rosal, C. G.; McCord, J. P.; Strynar, M. J.; Lindstrom, A. B.; Bergman, E. L.; Goodrow, S. M.; Tadesse, H. K.; Pilant, A. N.; Washington, B. J.; et al. Nontargeted mass-spectral detection of chloroperfluoropolyether nonoxylates in New Jersey soils. *Science* **2020**, *368* (6495), 1103–1107.
- (7) Munoz, G.; Liu, J.; Vo Duy, S.; Sauvé, S. Analysis of F-53B, Gen-X, ADONA, and emerging fluoroalkylether substances in environmental and biomonitoring samples: A review. *Trends Environ. Anal. Chem.* **2019**, *23*, e00066.
- (8) Rice, P. A.; Cooper, J.; Koh-Fallet, S. E.; Kabadi, S. V. Comparative analysis of the physicochemical, toxicokinetic, and

- toxicological properties of ether-PFAS. *Toxicol. Appl. Pharmacol.* **2021**, *422*, 115531.
- (9) Wang, Z.; Buser, A. M.; Cousins, I. T.; Demattio, S.; Drost, W.; Johansson, O.; Ohno, K.; Patlewicz, G.; Richard, A. M.; Walker, G. W.; et al. A new OECD definition for per- and polyfluoroalkyl substances. *Environ. Sci. Technol.* **2021**, *55* (23), 15575–15578.
- (10) FACT SHEET: Biden-Harris Administration Takes New Action to Protect Communities from PFAS Pollution. 2023. <https://www.whitehouse.gov/briefing-room/statements-releases/2023/03/14/fact-sheet-biden-harris-administration-takes-new-action-to-protect-communities-from-pfas-pollution/> (accessed 2023-03-14).
- (11) Proposed PFAS National Primary Drinking Water Regulation. 2023. <https://www.epa.gov/sdwa/and-polyfluoroalkyl-substances-pfas> (accessed 2023-06-06).
- (12) Wang, S.; Huang, J.; Yang, Y.; Hui, Y.; Ge, Y.; Larssen, T.; Yu, G.; Deng, S.; Wang, B.; Harman, C. First report of a Chinese PFOS alternative overlooked for 30 years: its toxicity, persistence, and presence in the environment. *Environ. Sci. Technol.* **2013**, *47* (18), 10163–10170.
- (13) Pan, Y.; Zhang, H.; Cui, Q.; Sheng, N.; Yeung, L. W.; Sun, Y.; Guo, Y.; Dai, J. Worldwide distribution of novel perfluoroether carboxylic and sulfonic acids in surface water. *Environ. Sci. Technol.* **2018**, *52* (14), 7621–7629.
- (14) Ruan, T.; Lin, Y.; Wang, T.; Liu, R.; Jiang, G. Identification of novel polyfluorinated ether sulfonates as PFOS alternatives in municipal sewage sludge in China. *Environ. Sci. Technol.* **2015**, *49* (11), 6519–6527.
- (15) Shi, Y.; Vestergren, R.; Xu, L.; Zhou, Z.; Li, C.; Liang, Y.; Cai, Y. Human exposure and elimination kinetics of chlorinated polyfluoroalkyl ether sulfonic acids (Cl-PFESAs). *Environ. Sci. Technol.* **2016**, *50* (5), 2396–2404.
- (16) Liu, S.; Jin, B.; Arp, H. P. H.; Chen, W.; Liu, Y.; Zhang, G. The fate and transport of chlorinated polyfluorinated ether sulfonates and other PFAS through industrial wastewater treatment facilities in China. *Environ. Sci. Technol.* **2022**, *56* (5), 3002–3010.
- (17) Joudan, S.; Mabury, S. A. Aerobic biotransformation of a novel highly functionalized polyfluoroether-based surfactant using activated sludge from a wastewater treatment plant. *Environ. Sci.: Process. Impacts* **2022**, *24* (1), 62–71.
- (18) Li, Y.; Yao, J.; Pan, Y.; Dai, J.; Tang, J. Trophic behaviors of PFOA and its alternatives perfluoroalkyl ether carboxylic acids (PFECAs) in a coastal food web. *J. Hazard. Mater.* **2023**, *452*, 131353.
- (19) Bentel, M. J.; Yu, Y.; Xu, L.; Kwon, H.; Li, Z.; Wong, B. M.; Men, Y.; Liu, J. Degradation of perfluoroalkyl ether carboxylic acids with hydrated electrons: structure–reactivity relationships and environmental implications. *Environ. Sci. Technol.* **2020**, *54* (4), 2489–2499.
- (20) Vasilyeva, T. P.; Karimova, N. M.; Slavich, Y. V. Synthesis of fluorine-containing benzimidazole derivatives. *Russ. Chem. Bull.* **2010**, *59* (1), 186–191.
- (21) Zhang, C.; Hopkins, Z. R.; McCord, J.; Strynar, M. J.; Knappe, D. R. U. Fate of per- and polyfluoroalkyl ether acids in the total oxidizable precursor assay and implications for the analysis of impacted water. *Environ. Sci. Technol. Lett.* **2019**, *6* (11), 662–668.
- (22) Che, S.; Jin, B.; Liu, Z.; Yu, Y.; Liu, J.; Men, Y. Structure-Specific Aerobic Defluorination of Short-Chain Fluorinated Carboxylic Acids by Activated Sludge Communities. *Environ. Sci. Technol. Lett.* **2021**, *8* (8), 668–674.
- (23) Yu, Y.; Che, S.; Ren, C.; Jin, B.; Tian, Z.; Liu, J.; Men, Y. Microbial defluorination of unsaturated per- and polyfluorinated carboxylic acids under anaerobic and aerobic conditions: A structure specificity study. *Environ. Sci. Technol.* **2022**, *56* (8), 4894–4904.
- (24) White, G. F.; Russell, N. J.; Tidswell, E. C. Bacterial scission of ether bonds. *Microbiol. Rev.* **1996**, *60* (1), 216–232.
- (25) Vainberg, S.; McClay, K.; Masuda, H.; Root, D.; Condee, C.; Zylstra, G. J.; Steffan, R. J. Biodegradation of Ether Pollutants by *Pseudonocardia* sp. Strain ENV478. *Appl. Environ. Microbiol.* **2006**, *72* (8), 5218–5224.
- (26) Steffan, R. J.; McClay, K.; Vainberg, S.; Condee, C. W.; Zhang, D. Biodegradation of the gasoline oxygenates methyl tert-butyl ether, ethyl tert-butyl ether, and tert-amyl methyl ether by propane-oxidizing bacteria. *Appl. Environ. Microbiol.* **1997**, *63* (11), 4216–4222.
- (27) Pearce, B. A.; Heydeman, M. T. Metabolism of di(ethylene glycol) [2-(2'-hydroxyethoxy)ethanol] and other short poly(ethylene glycol)s by gram-negative bacteria. *Microbiology* **1980**, *118* (1), 21–27.
- (28) Hur, H.; Newman, L. M.; Wackett, L. P.; Sadowsky, M. J. Toluene 2-monooxygenase-dependent growth of *Burkholderia cepacia* G4/PR1 on diethyl ether. *Appl. Environ. Microbiol.* **1997**, *63* (4), 1606–1609.
- (29) Moreno Horn, M.; Garbe, L.-A.; Tressl, R.; Adrian, L.; Görisch, H. Biodegradation of bis(1-chloro-2-propyl) ether via initial ether scission and subsequent dehalogenation by *Rhodococcus* sp. strain DTB. *Arch. Microbiol.* **2003**, *179* (4), 234–241.
- (30) McClay, K.; Schaefer, C. E.; Vainberg, S.; Steffan, R. J. Biodegradation of Bis(2-Chloroethyl) Ether by *Xanthobacter* sp. Strain ENV481. *Appl. Environ. Microbiol.* **2007**, *73* (21), 6870–6875.
- (31) Badenhop, J.; Weinholt, F. Natural steric analysis: Ab initio van der Waals radii of atoms and ions. *J. Chem. Phys.* **1997**, *107* (14), 5422–5432.
- (32) Liu, Z.; Bentel, M. J.; Yu, Y.; Ren, C.; Gao, J.; Pulikkal, V. F.; Sun, M.; Men, Y.; Liu, J. Near-quantitative defluorination of perfluorinated and fluorotelomer carboxylates and sulfonates with integrated oxidation and reduction. *Environ. Sci. Technol.* **2021**, *55* (10), 7052–7062.
- (33) Jin, B.; Liu, H.; Che, S.; Gao, J.; Yu, Y.; Liu, J.; Men, Y. Substantial defluorination of polychlorofluorocarboxylic acids triggered by anaerobic microbial hydrolytic dechlorination. *Nature Water* **2023**, *1* (5), 451–461.
- (34) Gao, J.; Liu, Z.; Chen, Z.; Rao, D.; Che, S.; Gu, C.; Men, Y.; Huang, J.; Liu, J. Photochemical degradation pathways and near-complete defluorination of chlorinated polyfluoroalkyl substances. *Nature Water* **2023**, *1* (4), 381–390.
- (35) Yang, S. H.; Shi, Y.; Strynar, M.; Chu, K. H. Desulfonation and defluorination of 6:2 fluorotelomer sulfonic acid (6:2 FTSA) by *Rhodococcus jostii* RHA1: Carbon and sulfur sources, enzymes, and pathways. *J. Hazard. Mater.* **2022**, *423*, 127052.
- (36) Cook, A. M.; Laue, H.; Junker, F. Microbial desulfonation. *FEMS Microbiol. Rev.* **1998**, *22* (5), 399–419.
- (37) Chen, Z.; Wang, X.; Dong, R.; Zhang, Y.; Jin, X.; Gu, C. Challenging the contamination of per- and polyfluoroalkyl substances in water: advanced oxidation or reduction? *Environmental Functional Materials* **2022**, *1* (3), 325–337.
- (38) Liu, Z.; Chen, Z.; Gao, J.; Yu, Y.; Men, Y.; Gu, C.; Liu, J. Accelerated degradation of perfluorosulfonates and perfluorocarboxylates by UV/sulfite + iodide: Reaction mechanisms and system efficiencies. *Environ. Sci. Technol.* **2022**, *56* (6), 3699–3709.
- (39) Gao, J.; Liu, Z.; Bentel, M. J.; Yu, Y.; Men, Y.; Liu, J. Defluorination of Omega-Hydroperfluorocarboxylates (omega-HPFCAs): Distinct Reactivities from Perfluoro and Fluorotelomeric Carboxylates. *Environ. Sci. Technol.* **2021**, *55* (20), 14146–14155.
- (40) Bentel, M. J.; Yu, Y.; Xu, L.; Li, Z.; Wong, B. M.; Men, Y.; Liu, J. Defluorination of Per- and Polyfluoroalkyl Substances (PFASs) with Hydrated Electrons: Structural Dependence and Implications to PFAS Remediation and Management. *Environ. Sci. Technol.* **2019**, *53* (7), 3718–3728.